physica status solidi

pss

www.pss-journals.com

reprint

WILEY-VCH

Phys. Status Solidi B **248**, No. 9, 2180–2185 (2011) / **DOI** 10.1002/pssb.201147015

physica status solidi b
www.pss-b.com
basic solid state physics

Large multiple resonance of magnetoelectric effect in a multiferroic composite cylinder with an imperfect interface

H. M. Wang[1], E. Pan[*,2,3], and W. Q. Chen[1]

[1] Department of Engineering Mechanics, Zhejiang University, Hangzhou 310027, P. R. China
[2] Computer Modeling and Simulation Group, University of Akron, Akron, OH 44325, USA
[3] School of Mechanical Engineering, Zhengzhou University, Zhengzhou, Henan 450001, P. R. China

Received 13 January 2011, revised 25 March 2011, accepted 29 March 2011
Published online 19 April 2011

Keywords cylindrical composites, magnetoelectric effect, multiple resonances, multiferroics

* Corresponding author: e-mail pan2@uakron.edu, Phone: 86-371-67739058, Fax: 86-371-67781786

The magnetoelectric (ME) effect in a bilayered piezoelectric/piezomagnetic cylinder with an imperfect interface under harmonic excitation is solved analytically. We show that while the interface imperfection would always reduce the static ME effect, the imperfect interface could play a significant positive role in enhancing the ME effect in the frequency domain >100 kHz. Combining with the curvature of the cylinder and the mechanical boundary conditions, we further demonstrate that it is possible to excite large ME effect at double and even multiple resonance frequencies, a unique feature which should be important to various microwave devices, such as antennas.

1 Introduction The magnetoelectric (ME) effect is defined as the ratio of the electric field output over the magnetic field input or *vice versa*. This coupling feature between the magnetic and electric fields can find important applications in various smart devices and systems, *e.g.* antennas, energy harvesters, magnetic sensors, current sensors, ME transformers, filters, phase shifters, and gradiometers [1–4]. While most single-phase multiferroic materials exhibit only a very weak ME effect, strong ME effects could be achieved by bonding a piezoelectric (PE) phase to a piezomagnetic (PM) one, the typical multiferroic composite. The ME effect in layered composite plates was investigated both analytically and experimentally [5–12]. The ME effect in PE/PM composites with other shapes, such as disk, cylinder and shell, was also reported [13–15]. Studies on multiferroic nanocomposites were further carried out [16, 17]. Several practical and efficient ways were proposed to enhance the ME effect, for instance, by changing the geometric parameter and mechanical conditions [18], using the resonance driving frequency [19], employing the functionally graded materials [20], altering the polarization direction [21], and by applying different magnetic bias field [22].

In fact, the ME effect in PE/PM composites is a product property. Thus, the coupling effect between the electric and magnetic fields in the PE/PM composites is mediated by the mechanical field through the interface. This indicates that the ME effect could be adjusted and/or tuned by the interface. Under a static deformation, Wang and Pan recently investigated the ME effect in multiferroic fibrous composites with imperfect interfaces [23]. They showed that as long as the interface is imperfect, the static ME effect of the composite, say the $BaTiO_3$-$CoFe_2O_4$ fibrous composite, would be always reduced. Since any real interface in the composite will involve certain degree of imperfection [23], the influence and/or role of the imperfect interface on the ME effect in multiferroic composite, under both static and time-harmonic deformations, becomes extremely critical.

Thus, in this article, we study the ME effect in a bilayer PE/PM composite cylinder with an imperfect interface subject to either a static or harmonic magnetic excitation. Following Wang et al. [24], we first derive an analytical solution for the ME effect in the composite with an imperfect interface and then we present some numerical results on these effects for given geometries and mechanical boundary conditions. It is striking that, while under static deformation,

an imperfect interface would always reduce the ME effect [23], it can positively affect the ME effect in the frequency domain >100 kHz. Depending on the boundary conditions and the curvature of the composite cylinder [24], we show that large ME effect can be achieved not only at the single resonance frequency, but also at double resonance frequencies with nearly equal amplitudes. A third resonance could be further observed when the interface property is properly tuned although its amplitude is small. These unique features should be of particular importance to device design, say antennas, so that it can operate under multiple resonance [25].

2 Problem description and solutions The bilayer multiferroic composite cylinder to be studied is shown in Fig. 1, similar to that used in experiment [26]. The radius of each surface, from the inner to the outer, is denoted by a, b, and c, respectively. The inner layer is made of PM with a mass density ρ_{m} and the outer PE with ρ_{e}. The PE layer is polarized in the radial direction and is shorted at its inner surface $r=b$. We assume that the composite is driven by a time harmonic uniform radial magnetic field $H_0\exp(i\omega t)$ [26], where H_0 is a known constant, $i=\sqrt{-1}$ the imaginary unit, ω the driving circular frequency, and t the time variable. For a harmonic motion, all the field quantities will have the same time-dependent factor $\exp(i\omega t)$, which will be dropped for the sake of brevity in the analysis. In the polar coordinate system (r,θ) all the field variables are functions of r only for the long cylinder case. In other words, a plane-strain deformation in the (r,θ)-plane is assumed. We further introduce the following quantities and material properties: Φ is the electric potential, u_{r} the radial elastic displacement and σ_{rr} the radial normal stress; c_{ij}, ε_{ij}, e_{ij}, and q_{ij} are the elastic, dielectric, PE, and PM coefficients, respectively.

The general "plane-strain" solution for the elastic displacement in the radial direction in the PM layer can be found as [24]

$$u_r(\omega,r) = A_m J_{\mu_m}(k_m r) + B_m Y_{\mu_m}(k_m r) + H_0 G(\omega,r), \qquad (1)$$

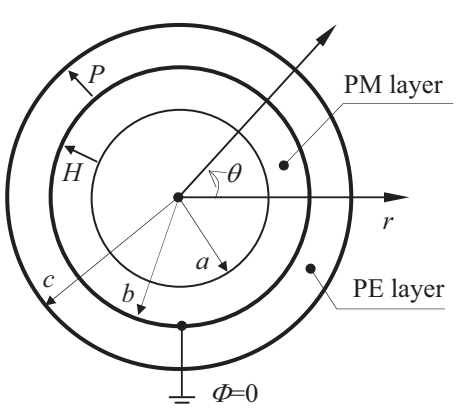

Figure 1 Schematic of bilayer PE/PM cylindrical composite with H being the radial magnetic field and P the radial polarization.

where

$$k_m = \frac{\omega}{c_m}, \quad c_m = \sqrt{\frac{c_{33}}{\rho_m}}, \quad \mu_m = \sqrt{\frac{c_{11}}{c_{33}}}. \qquad (2)$$

Also in Eq. (1), A_m and B_m are two unknown coefficients to be determined; $J_{\mu_m}(\cdot)$ and $Y_{\mu_m}(\cdot)$ are the first and second kind Bessel functions of order μ_m, and

$$G(\omega,r) = QS_{0,\mu_m}(k_m r), \qquad (3)$$

where $Q=(q_{33}-q_{31})/c_{33}$, and $S_{0,\mu_m}(k_m r)$ is the Lommel function which can be written in terms of the Bessel functions as

$$S_{0,\mu_m}(k_m r) = \frac{\pi}{2}\left[Y_{\mu_m}(k_m r)\int_a^r J_{\mu_m}(k_m\xi)\mathrm{d}\xi - J_{\mu_m}(k_m r)\int_a^r Y_{\mu_m}(k_m\xi)\mathrm{d}\xi\right]. \qquad (4)$$

Similarly, the general solution of the elastic displacement in the radial direction in the PE layer is

$$u_r(\omega,r) = A_e J_{\mu_e}(k_e r) + B_e Y_{\mu_e}(k_e r), \qquad (5)$$

where A_e and B_e are coefficients to be determined, and

$$k_e = \frac{\omega}{c_e}, \quad c_e = \sqrt{\frac{\bar{c}_{33}}{\rho_e}}, \quad \mu_e = \sqrt{\frac{\bar{c}_{11}}{\bar{c}_{33}}}, \qquad (6)$$

with

$$\begin{aligned} \bar{c}_{33} &= c_{33} + e_{33}e_3, \\ \bar{c}_{11} &= c_{11} + e_{31}e_1, \\ \bar{c}_{13} &= c_{13} + e_{31}e_3; \end{aligned} \qquad (7)$$

$$e_1 = e_{31}/\varepsilon_{33}, \; e_3 = e_{33}/\varepsilon_{33}. \qquad (8)$$

If the driving frequency $\omega=0$, we then have $k_{\mathrm{m}}=0$ in Eq. (2) for the PM layer and $k_{\mathrm{e}}=0$ in Eq. (6) for the PE layer. Thus the corresponding static solution can be reduced from Eqs. (1) and (5).

On the inner and outer surfaces of the composite cylinder, we consider the following four sets of mechanical boundary conditions (MBCs) [24]: (i) Both the inner and outer surfaces are traction free (F–F) $\sigma_{\mathrm{rr}}(a)=\sigma_{\mathrm{rr}}(c)=0$; (ii) The inner surface is clamped while the outer surface is traction free (C–F) $u_r(a)=\sigma_{\mathrm{rr}}(c)=0$; (iii) The inner surface is traction free while the outer surface is clamped (F–C) $\sigma_{\mathrm{rr}}(a)=u_r(c)=0$; and (iv) Both the inner and outer surfaces are clamped (C–C) $u_r(a)=u_r(c)=0$. In order to model possible defects/damages on the interface or to simulate a thin glue layer between the PE and PM phases, we adopt the following spring layer model [23, 27, 28] for the interfacial behavior:

$$\sigma_{\mathrm{rr}}(b_+) = \sigma_{\mathrm{rr}}(b_-) = [u_r(b_+)-u_r(b_-)]/\chi, \qquad (9)$$

where b_+ denotes the surface of the PE layer at $r = b$ and b_- that of the PM layer; and χ is the interfacial parameter (compliance). It is noted that $\chi = 0$ corresponds to a perfectly bonded interface.

For given MBCs, along with the imperfect interface condition, the four unknowns A_e, B_e, A_m, and B_m can be determined. To calculate the ME effect, the average electric field in the PE layer is adopted. When the outer surface of the PE layer is open circuited, the gradient of the electric potential in the PE layer can be derived as $d\Phi/dr = e_3 du_r/dr + e_1 r^{-1} u_r$. Integrating this expression over the spatial interval $[b, c]$ and using the inner surface of the PE layer as reference (*i.e.*, we assume that this surface is electrically shorted $\Phi|_{r=b} = 0$), we obtain the voltage difference between the inner and outer surfaces of the PE layer as

$$\Phi_{bc} = e_3\left(u_r|_{r=c} - u_r|_{r=b}\right) + e_1 \int_b^c r^{-1} u_r(r) dr. \tag{10}$$

We thus define the ME effect as

$$\alpha = \Phi_{bc}/(tH_0), \tag{11}$$

where $t = c - a$ is the total thickness of the composite [18].

3 Influence of imperfect interface on the ME effect With the derived analytical solution, we can now study the impact of the imperfect interface on the ME effect for different MBCs as well as geometric and material parameters. In our numerical examples for the bilayer PE/PM composite cylinder with an imperfect interface, we use $CoFe_2O_4$ (CFO) and PZT-5A (PZT) for the PM and PE phases, respectively. All the material parameters are taken from Ref. [29] and are listed in Table 1.

Table 1 Material properties of PZT-5A (PZT) and $CoFe_2O_4$ (CFO) [29] (C_{ij}: elastic constants in GPa; e_{ij}: PE coefficients in N/(Vm); q_{ij}: PM coefficients in N/(Am); ε_{ij}: permittivity coefficients in 10^{-8} C/(Vm); μ_{ij}: permeability coefficients in 10^{-6} Wb/(Am); and ρ: density in 10^3 kgm^{-3}).

	PZT	CFO		PZT	CFO
C_{11}	99.201	286	q_{31}	0	580.3
C_{13}	50.778	170.5	q_{33}	0	699.7
C_{33}	86.856	269.5	ε_{33}	1.5	–
e_{31}	−7.209	0	μ_{33}	–	157
e_{33}	15.118	0	ρ	7.75	5.3

We first consider the effect of the imperfect interfacial property on the static ME effect in the PE/PM cylindrical composite. In this example, the thickness of the composite is taken as $t = 20$ mm and the inner radius $a = 30$ mm and $a = 80$ mm. Two dimensionless quantities are introduced to illustrate the results: One is the thickness ratio m and the other the dimensionless parameter of the interfacial compliance λ.

$$m = t_e/t, \quad \lambda = \chi/\chi_0, \tag{12}$$

where t_e is the thicknesses of the PE layer and $\chi_0 = t/c_{33}^*$ with c_{33}^* being the elastic constant c_{33} of the PE layer.

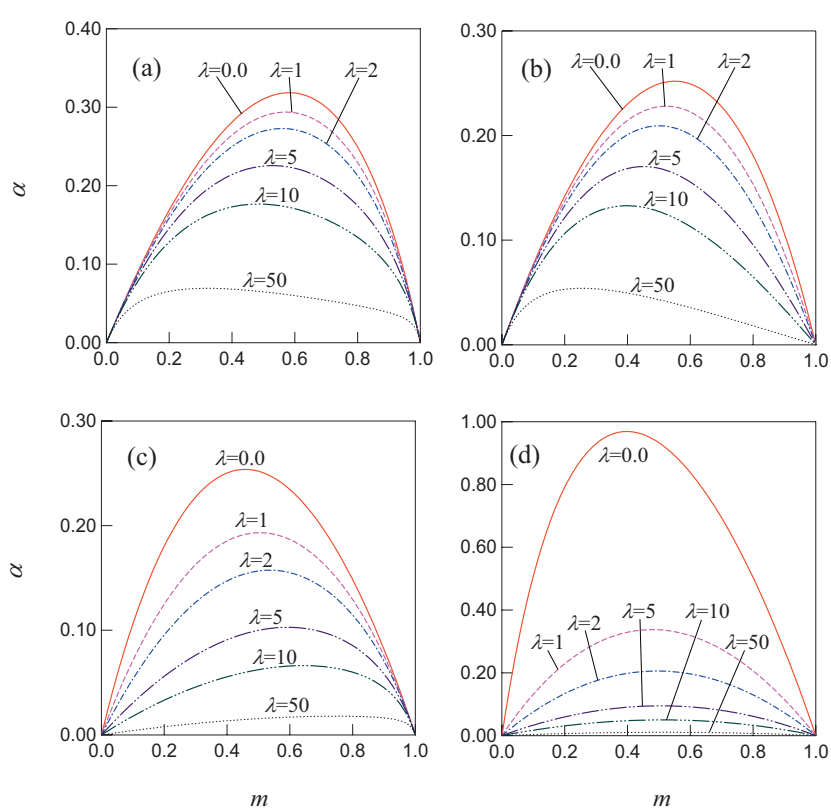

Figure 2 (online color at: www.pss-b.com) Variation of ME effect α *versus* thickness ratio m for $a = 30$ mm: (a) F–F; (b) C–F; (c) F–C; (d) C–C. The unit of α is (V/m)(A/m)$^{-1}$.

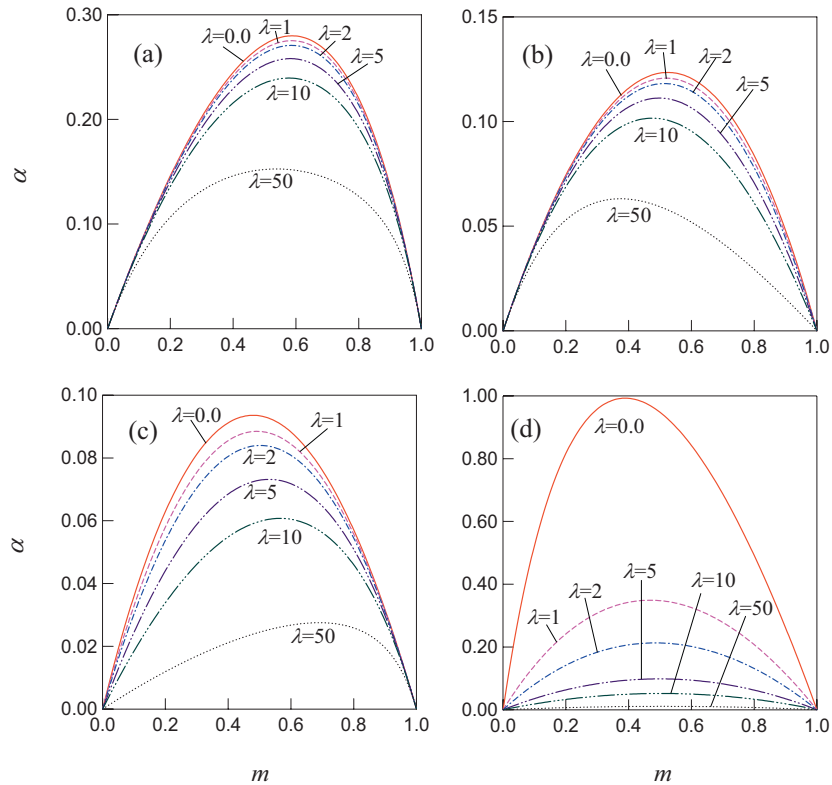

Figure 3 (online color at: www.pss-b.com) Variation of ME effect α *versus* thickness ratio m for $a = 80$ mm: (a) F–F; (b) C–F; (c) F–C; (d) C–C. The unit of α is (V/m)(A/m)$^{-1}$.

Figures 2 and 3 show the variation of the ME effect with respect to the thickness ratio m for the PE/PM composite cylinder of inner radius $a = 30$ mm and $a = 80$ mm with an imperfect interface. These curves show that: (i) For all four sets of MBCs, the ME effect α decreases with increasing interface parameter λ (*i.e.*, when the interface becomes weak), a feature consistent with existing report [23]. (ii) For the perfect interface $\lambda = 0$, the ME effect for the C–C MBC is always larger than that for the other three MBCs. Such phenomenon agrees well with previous experimental and analytical reports [7, 18]. (iii) As λ increases, the ME effect under the C–C MBC experiences a sharp decrease. It drops 3–4 times in magnitude when the interface behavior changes from a perfect interface ($\lambda = 0$) to an imperfect one ($\lambda \neq 0$). We have calculated the ME effect for other inner radius values and found that comparing with the C–F and F–C MBCs, the ME effect for the F–F and C–C MBCs is relatively insensitive to the inner radius.

We next consider the ME effect in the PE/PM composite under harmonic driving. In our calculation, the elastic constants of the PE and PM layers are multiplied by a complex factor $(1 + 0.05\mathrm{i})$ to account for the damping [30]. We further fix the thickness of the PE layer at $t_e = 10$ mm and the thickness ratio at $m = 0.5$ (the ratio near which we observe a large ME effect under static deformation).

Figures 4 and 5 show the ME effect as a function of the driving frequency. The peaks reveal that a large ME effect can be achieved when the composite is driven by an excitation near the resonance frequency. It is observed that for all four sets of MBCs, the ME effect increases slightly when the inner radius is changed from $a = 30$ to 80 mm. Actually, we have further increased the inner radius a and found that the increase in the ME effect was only moderate. From Figs. 4 and 5, the following remarkable features are observed: (i) In contrast to the static case, the ME effect at the resonant frequencies has nearly the same magnitude under different MBCs, except for the F–C MBC where its ME effect magnitude at peak frequencies is only about half of other MBCs. (ii) At some special resonance frequencies, the imperfect interface can actually enhance the ME effect in the composites, a feature totally different from the static case where the imperfect interface would always reduce the ME effect. In other words, the imperfect parameter could provide an alternative avenue to enhance the ME effect in the PE/PM composite. (iii) While the C–C MBC is always associated with a single resonance, a common feature which was frequently reported (e.g., [31]), other MBCs can be applied to excite double and even triple resonances with nearly identical amplitude (at least at two separate resonant frequencies). This latter feature is due to the special interaction between the PE and PM layers via the mechanical strain, and could be extremely useful in the design of microwave devices (like antennas), so that they can efficiently operate simultaneously at multiple frequencies [25]. (iv) While different MBCs can be utilized to tune the resonance at different frequencies, the imperfect interface parameter can be employed to either generate additional resonance (like C–F MBC) or annul the small frequency peak (like C–C MBC).

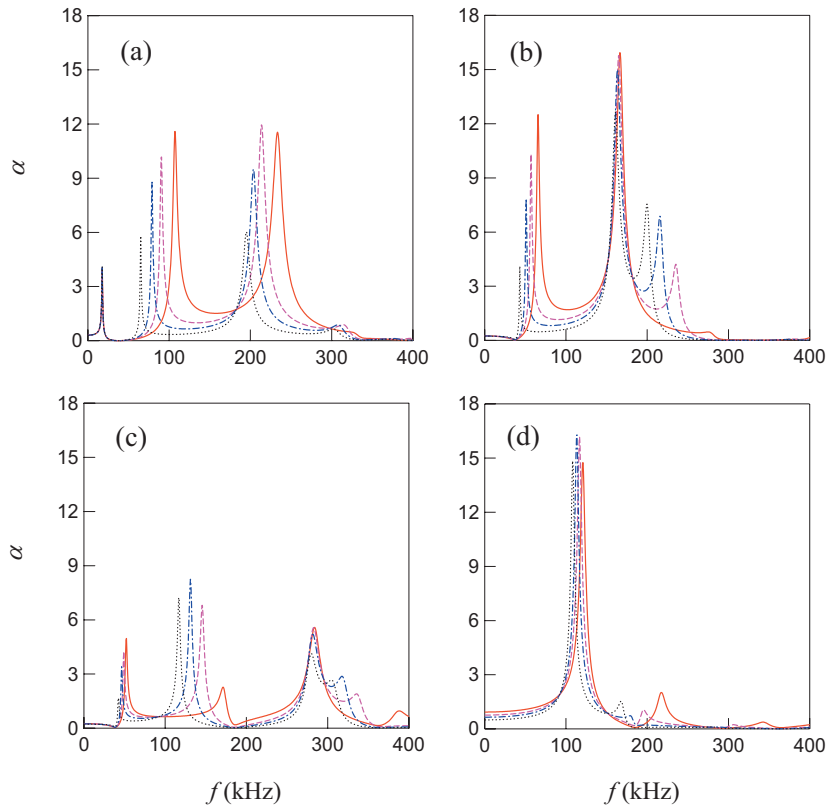

Figure 4 (online color at: www.pss-b.com) Variation of ME effect α *versus* driving frequency for $a = 30$ mm and $m = 0.5$. (a) F–F; (b) C–F; (c) F–C; (d) C–C. Interface parameter $\lambda = 0.0$ (red solid line), 0.125 (pink dashed line), 0.25 (blue dash-dotted line), 0.5 (black dotted line). The unit of α is (V/m)(A/m)$^{-1}$.

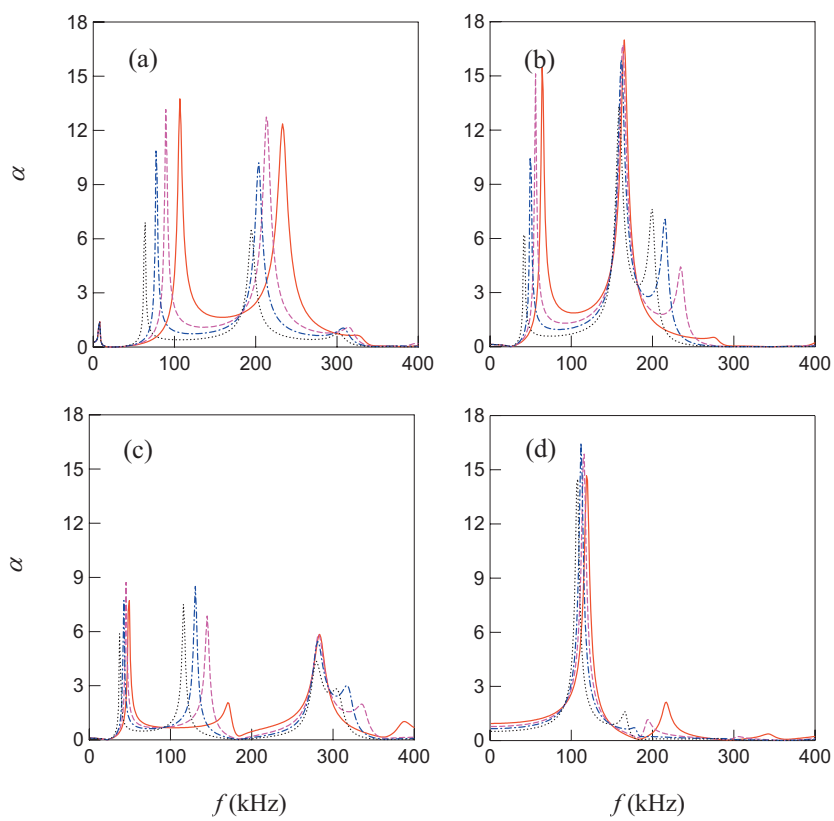

Figure 5 (online color at: www.pss-b.com) Variation of ME effect α *versus* driving frequency for $a = 80$ mm and $m = 0.5$. (a) F–F; (b) C–F; (c) F–C; (d) C–C. Interface parameter $\lambda = 0.0$ (red solid line), 0.125 (pink dashed line), 0.25 (blue dash-dotted line), 0.5 (black dotted line). The unit of α is (V/m)(A/m)$^{-1}$.

4 Conclusions By deriving an analytical solution for a PE/PM cylinder with an imperfect interface, we studied the ME effect in this bilayer multiferroic composite. It is shown that the mechanical boundary conditions, interface properties, and the curvature of the cylinder combined together can remarkably affect the ME coupling coefficient. In particular, we have demonstrated that under a time-harmonic magnetic field input, an imperfect interface in the composite cylinder can not only enhance the resonance of the ME effect, but also generate additional resonance with large amplitude or annul small unwanted resonance for better device operation. Our results clearly indicate alternative avenues for designing ME effect-based devices, such as antennas, so that they can operate at multiple resonance with equal amplitudes.

Acknowledgements The work was supported by National Natural Science Foundation of China (Nos. 10872179, 10725210, and 10832009), Zhejiang Provincial Natural Science Foundation of China (No. Y7080298), Zhejiang Provincial Innovation Teams (No. 2009R50025) and Xinxing Plans of Zhejiang University, and by Henan Province via Bairen Program.

References

[1] S. Priya, R. Islam, S. X. Dong, and D. Vehland, J. Electroceram. **19**, 149 (2007).
[2] C. S. Park, C. W. Ahn, J. Ryu, W. H. Yoon, D. S. Park, H. E. Kim, and S. Priya, J. Appl. Phys. **105**, 094111 (2009).
[3] P. Li, Y. M. Wen, P. A. Liu, X. S. Li, and C. B. Jia, Sens. Actuators A **157**, 100 (2010).
[4] C. L. Zhang, J. S. Yang, and W. Q. Chen, Appl. Phys. Lett. **95**, 013511 (2009).
[5] J. Ryu, A. V. Carazo, K. Uchino, and H. Kim, Jpn. J. Appl. Phys. **40**, 4948 (2001).
[6] M. I. Bichurin, V. M. Petrov, and G. Srinivasan, J. Appl. Phys. **92**, 7681 (2002).
[7] M. I. Bichurin, V. M. Petrov, and G. Srinivasan, Phys. Rev. B **68**, 054402 (2003).
[8] J. G. Wan, J. M. Liu, H. L. W. Chand, C. L. Choy, G. H. Wang, and C. W. Nan, J. Appl. Phys. **93**, 9916 (2003).
[9] S. Dong, J. F. Li, and D. Viehland, IEEE Trans. Ultrason. Ferroelectr. Freq. Control **50**, 1253 (2003); IEEE Trans. Ultrason. Ferroelectr. Freq. Control **51**, 793 (2004).
[10] J. X. Zhang, Y. L. Li, D. G. Schlom, L. Q. Chen, F. Zavaliche, R. Ramesh, and Q. X. Jia, Appl. Phys. Lett. **90**, 052909 (2007).
G. Srinivasan, Annu. Rev. Mater. Res. **40**, 153 (2010).
[11] Z. Huang, J. Appl. Phys. **100**, 114104 (2006).
[12] C. L. Zhang, W. Q. Chen, J. Y. Li, and J. S. Yang, IEEE Trans. Ultrason. Ferroelectr. Freq. Control **56**, 1046 (2009).
[13] D. A. Filippov, Tech. Phys. Lett. **30**, 983 (2004).
[14] C. L. Zhang, J. S. Yang, and W. Q. Chen, Int. J. Appl. Electromagn. Mech. **28**, 441 (2008).
D. A. Pan, Y. Bai, A. A. Volinsky, W. Y. Chu, L. J. Qiao, Appl. Phys. Lett. **92**, 052904 (2008).
[15] Y. Benveniste, Phys. Rev. B **51**, 16424 (1995).
J. Y. Li, M. L. Dunn, J. Intell. Mater. Syst. Struct. **9**, 404 (1998).
[16] V. M. Petrov, G. Srinivasan, M. I. Bichurin, and A. Gupta, Phys. Rev. B **75**, 224407 (2007).
[17] E. Pan, X. Wang, and R. Wang, Appl. Phys. Lett. **95**, 181904 (2009).
[18] E. Pan and R. Wang, J. Phys. D **42**, 245503 (2009).
[19] M. I. Bichurin, D. A. Filippov, V. M. Petrov, V. M. Laletsin, N. Paddubnaya, and G. Srinivasan, Phys. Rev. B **68**, 132408 (2003).
[20] V. M. Petrov and G. Srinivasan, Phys. Rev. B **78**, 184421 (2008).
X. Wang, E. Pan, J. D. Albrecht, and W. J. Feng, Compos. Struct. **87**, 206 (2009).
[21] S. X. Dong, J. F. Li, and D. Viehland, Appl. Phys. Lett. **84**, 4188 (2004).
[22] S. S. Guo, S. G. Lu, Z. Xu, X. Z. Zhao, and S. W. Or, Appl. Phys. Lett. **88**, 182906 (2006).
[23] X. Wang and E. Pan, Phys. Rev. B **76**, 214107 (2007).
[24] H. M. Wang, E. Pan, and W. Q. Chen, J. Appl. Phys. **107**, 093514 (2010).
[25] K. Tsunekawa and S. Hagiwara, United States Patent 5568155 (1996).
I. Pankinaho, United States Patent 6140966 (2000).
H. Greim, V. Matschi, United States Patent 7570059 B2 (2009).
D. de Cogan, and A. Alani, Electron. Lett. **21**, 1153 (1985).
J. Lou, M. Liu, D. Reed, Y. Ren, and N. X. Sun, Adv. Mater. **21**, 4711 (2009).
C. E. Ciomaga, I. Dumitru, L. Mitoseriu, C. Galassi, A. R. Iordan, M. Airimioaei, and M. N. Palamaru, Scr. Mater. **62**, 610 (2010).
[26] D. A. Pan, Y. Bai, W. Y. Chu, and L. J. Qiao, J. Phys. D, Appl. Phys. **41**, 022002 (2008).
[27] M. Rajabi and S. M. Hasheminejad, Ultrasonics **49**, 682 (2009).
[28] W. Q. Chen, Y. F. Wang, J. B. Cai, and G. R. Ye, Int. J. Solids Struct. **41**, 2429 (2004).
[29] E. Pan, ASME J. Appl. Mech. **68**, 608 (2001).
F. Ramirez, P. R. Heyliger, and E. Pan, J. Sound Vib. **292**, 626 (2006).
[30] C. L. Zhang, W. Q. Chen, J. Y. Li, and J. S. Yang, Smart Mater. Struct. **18**, 095026 (2009).
[31] C. W. Nan, M. I. Bichurin, S. X. Dong, D. Viehland, and G. Srinivasan, J. Appl. Phys. **103**, 031101 (2008).